Temperate Mountain Glacier-Melting Rates for the Period 2001–30: Estimates from Three Coupled GCM Simulations for the Greater Himalayas

DIANDONG REN, DAVID J. KAROLY, AND LANCE M. LESLIE

School of Meteorology, University of Oklahoma, Norman, Oklahoma

(Manuscript received 14 March 2006, in final form 10 October 2006)

ABSTRACT

The temperate glaciers in the greater Himalayas (GH) and the neighboring region contribute to the freshwater supply for almost one-half of the people on earth. Under global warming conditions, the GH glaciers may melt more rapidly than high-latitude glaciers, owing to the coincidence of the accumulation and ablation seasons in summer. Based on a first-order energy balance approach for glacier thermodynamics, the possible imposed additional melting rate was estimated from three climate simulations using the Geophysical Fluid Dynamics Laboratory Global Coupled Climate Model version 2.1 (GFDL-CM2.1), the Model for Interdisciplinary Research on Climate 3.2, high-resolution version (MIROC3.2-hires), and the Met Office's Third Hadley Centre Coupled Ocean–Atmosphere General Circulation Model (HadCM3). The simulations were carried out under the Special Report on Emissions Scenarios (SRES) A1B scenario. For the 30-yr period of 2001–30, all three CGCMs indicate that the glacial regions most sensitive to regional warming are the Tianshan–Altai Mountains to the north and Hengduan Mountains to the south. A map of potential melting was produced and was used to calculate the glacier-melting speed, yielding an additional spatially averaged glacier depth reduction of approximately 2 m for the 2001–30 period for those areas located below 4000 m. Averaged over the entire GH region, the melting rate is accelerating at about 5 mm yr^{-2}. The general circulation over the GH region was found to have clear multidecadal variability, with the 30-yr period of 2001–30 likely to be wetter than the previous 30-yr period of 1971–2000. Considering the possible trend in precipitation from snow to rain, the actual melting rates of the GH glaciers may even be larger than those obtained in this research.

1. Introduction

Climate change and its wide range of possible impacts have been recurring topics in both the refereed scientific literature and in the popular media. Coupled general circulation models (CGCMs) require only a small number of external boundary conditions, such as the solar constant and the atmospheric concentrations of radiatively active gases and aerosols, to simulate the physical climate system. They have been employed for decades in theoretical investigations of the mechanisms of climate change. In this study, CGCMs are used to estimate future anthropogenic climate changes and the ensuing changes in the melting rate of the greater Himalayan (GH) glaciers. The perennial snow and ice cover of the GH glaciers makes up a huge freshwater store located in an otherwise arid, drought-prone region. Glacial meltwaters make a major contribution to the flow of several major river systems and to the livelihood of about half of the people on earth (Shi 2001).

Our interest therefore focuses on regional climate change implications for the GH, a region spanning 25°–45°N, 70°–105°E. The GH includes the Qinghai–Xizhang Plateau and the Tianshan–Altai Mountains in the north. This region is an important component of the central Asian mountain system, largely because it has the greatest concentration of glaciers (in number density) outside the polar caps, and is representative of midlatitude mountain/valley glaciers. For example, the Himalayas have a glacier coverage of 33 000 km^2 and provide around 5.04×10^{10} m^3 of water annually (Sheng and Chen 1996; Dyurgerov and Meier 1997), and the glacier number density for the middle Tianshan area is greater than 150 glaciers per 1000 square kilometers (B. Li 2005, personal communication).

Climate change, whether natural or human induced, has already impacted this glacier ecosystem tremen-

Corresponding author address: Dr. Diandong Ren, School of Meteorology, University of Oklahoma, 100 East Boyd, Norman, OK 73019.
E-mail: dd_ren@rossby.metr.ou.edu

DOI: 10.1175/JAM2499.1

dously. About 67% of its glaciers are retreating at a startling rate in the GH, with the major causal factor identified as the regional temperature increase (Shi 2001; Ageta and Kadota 1992; Yamada et al. 1992). The fate of these and other mountain glaciers has received increasing attention in recent years (Thompson et al. 1997, 2000), partly from concerns that vital paleoclimate information may be lost permanently.

Owing to the remote, inaccessible, and inhospitable nature of the GH environment, field investigations of glaciers have been limited to a few individual glaciers in this area. Several recent studies have looked at glacier terminus fluctuations and glacier area changes as indicators of regional climate change, primarily using remote sensing and GIS techniques. Retreating rates greater than measurement uncertainty were identified and verified using runoff and meteorological observations. A shortcoming of the optical satellite remote sensing technique used for monitoring glaciers is that the thickness change and volume reduction cannot yet be measured with sufficient accuracy (Davis et al. 1998).

In addition, our focus is on the ensemble behavior of glaciers as a whole rather than individually. Coupled GCMs are valuable tools in that they can produce arbitrarily long, physically based atmospheric fields with full global coverage. Despite their significantly improved regional fidelity (Karoly and Wu 2005; Feddema et al. 2005), especially in precipitation (Lau and Yang 1996; Meehl and Arblaster 1998), the use of CGCMs to model glacier variations in the monsoonal region has been rare, largely resulting from the coarseness of the resolution of CGCMs.

In this study, based on the simulation of three CGCMs under the A1B scenario of the Special Report on Emissions Scenarios (SRES A1B; Houghton et al. 2001), two-dimensional maps of the additional melting rate caused by regional temperature increases were produced for the GH, using a simplified energy balance method.

2. Study region and data

Our specific interest in this study is the regional manifestation of global warming in central and temperate East Asia, over a region including the Tianshan–Altai Mountains and the Tibetan Plateau (Qinghai–Xizhang Plateau, see Fig. 1a). Luo and Yanai (1983) analyzed the onset of the monsoon in the 10°–50°N, 60°–130°E domain. They focused on the downstream and southern part of this domain. Here, we employ a similar domain [the Asian monsoon region (hereinafter the AM region)], shifted slightly to the north and covering the 15°–55°N, 60°–130°E region, because we are interested in the cold, arid region [approximately Region I of Luo and Yanai (1983)]. The equivalent resolution of the CGCM used here is relatively high, and we ensure that at least 50 grid points fall within the selected region. Land surface phenomena, such as glacier variation, experience the effects of environmental change locally, rather than as an average value over a wide region. However, the model fidelity may diminish if too few grid points are included in the region of interest.

The selected regions are affected by the Asian monsoon system and their precipitation falls primarily during summer months (Ye 1981; Luo and Yanai 1983; Fu et al. 2002). For the central Asian region (e.g., the Tianshan region), winter precipitation, which contributes significantly to the glacier mass balance, may also be affected by the westerly disturbances originating in the inland seas and moving to the east. Glaciers in this region, when compared with those of the remaining regions, should exhibit a different response to a changing climate owing to their extreme continental nature, which gives rise to both aridity and large seasonal temperature variations, and also to the near coincidence of accumulation and ablation seasons in summer (Ageta and Higuchi 1984; Shi 2001; Fu et al. 2002). Hence, we use the mean summer temperatures from June to August as the climatic change index for studying the effect of climate change on mountain glaciers, with the understanding that the warming may well be more significant during the winter months.

At present, the most advanced models that include the interactions among the atmosphere, oceans, land, and ice–snow are CGCMs. Based on the ability of the models to reproduce twentieth-century climate and the fact that the astronomical boundary conditions have been relatively stable (Houghton et al. 2001) over the past 1000 yr, CGCM simulations can be used to identify regional-scale climate change and derive uncertainty measures for future climate change. The ensemble mean surface temperature predictions from nine CGCMs yield a good resemblance both to the Global Historical Climatology Network (GHCN) data (Peterson and Vose 1997) and the Hadley Centre Climate Research Unit (HadCRU; Folland et al. 2001) observations, especially during the past 50 yr. Our analysis of the ensembles reveals an increasing trend of 0.27°C (10 yr)$^{-1}$ for the June–August (JJA) temperature over the past 30 yr for the GH, which is in agreement with the ice core records from the Dasuopu Glacier of the Himalayas, in Tibet, which indicate that the last decade and the last 50 yr have been the warmest in the past 1000 yr (Thompson et al. 2000).

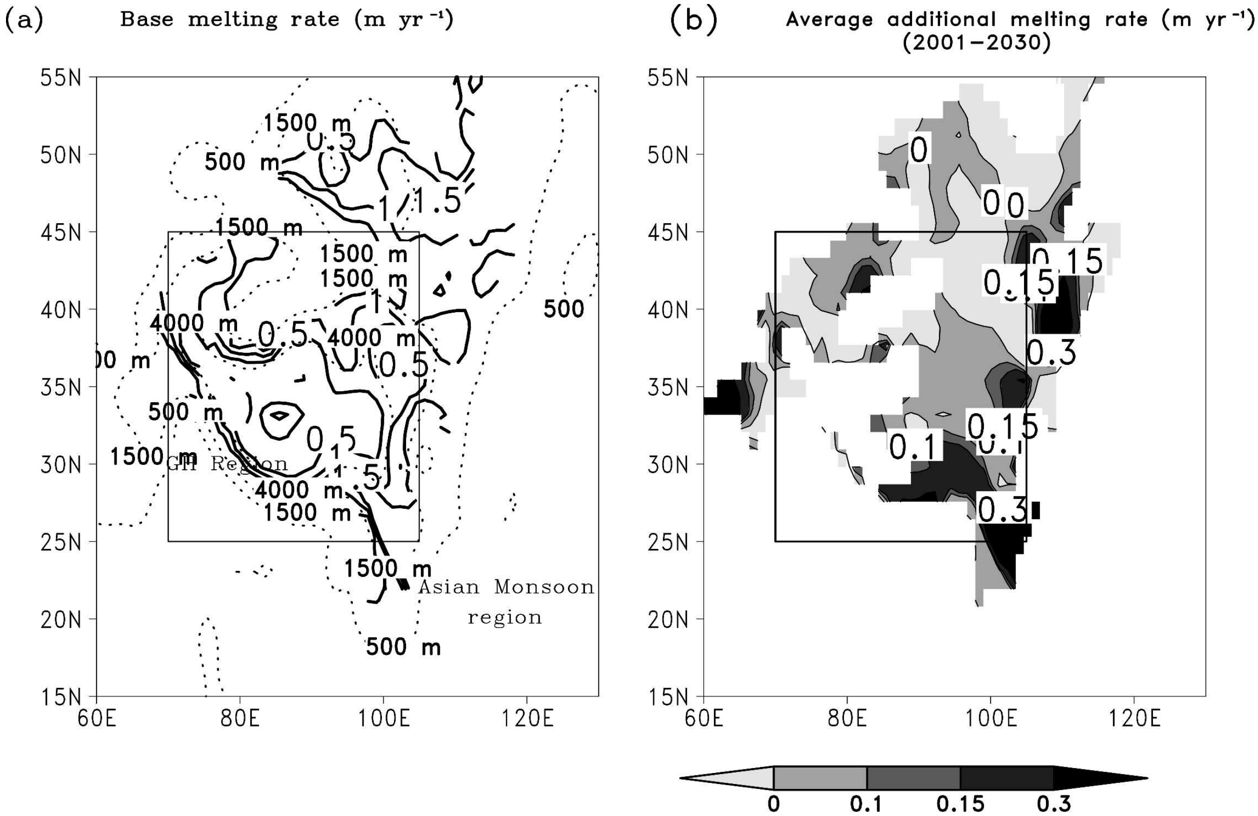

FIG. 1. (a) Base melting rate and (b) average additional melting rate (m yr^{-1}) for the Asian monsoon region over 2001–30, obtained using Eq. (2), with surface air temperature, skin temperature, surface air pressure, and wind speed obtained from MIROC3.2-hires simulations under SRES A1B scenario. Regions with JJA surface temperature larger than 297 K are masked out. In (a), thin dashed lines are topography (m). The small box outlines the Greater Himalayas.

Transient climate simulations under SRES A1B used in this research are obtained from the Program for Climate Model Diagnosis and Intercomparison (PCMDI) Coupled Model Intercomparison Project (CMIP; Gregory et al. 2005). The model variables used include monthly mean near-surface air temperature, a variable slated as the highest priority output fields in the CMIP project, the surface (skin) temperature, surface pressure, and the 2-m wind speed. We chose the Geophysical Fluid Dynamics Laboratory Global Coupled Climate Model, version 2.1 (GFDL-CM2.1; Delworth et al. 2006), the Model for Interdisciplinary Research on Climate 3.2, high-resolution version (MIROC3.2-hires; Kimoto 2005), and the Met Office's Third Hadley Centre Coupled Ocean–Atmosphere General Circulation Model (HadCM3; Gordon et al. 2000) primarily because they provide all of the input variables to our simple first-order glacier thermodynamic scheme described below.

The ultimate fate of the glaciers is determined by the new equilibrium temperature within the framework of global warming. The transient climate we will experience over the next century is critical in that it provides us with a chance to compare the predictions for different scenarios and provides a longer-term predictability that could prove to be valuable to minimizing the impact of increased mountain glacier melting. In this study, estimates of the warming effects on glacier melting are based on the SRES A1B scenario, which suggests a balanced energy source (between fossil fuels and other energy sources) for a future world of very rapid economic growth. For the upcoming 30 yr, its carbon dioxide emission is close to strong emission scenarios such as A2, but with significantly less sulfate loading. We chose the SRES A1B primarily because it reflects the most recent trends in driving forces of emissions: population projections, economic development, and structural and technological change (Houghton et al. 2001).

3. The glacier melt model

The key to glacier longevity is the solid mass balance, controlled by local energy balance (see the appendix) and solid precipitation. A definitive relationship between mass balance and the atmospheric parameters (such as short- and longwave radiation, air temperature, and solid precipitation) is not easy to find. Empirical degree-day models of ablation are often applied for individual glaciers and ice sheets (Raper and Braithwaite 2006; van der Veen 1999, p. 355). Degree-day models give satisfactory ablation simulations for equator-facing valley glaciers during periods with high correlations between net radiation and sensible heat (eddy) fluxes, and when sensible heat fluxes are less forced by stronger winds than by higher temperature. The traditional degree-day model was not suitable for using monthly data before the improvements made by Braithwaite (1984), which allow the positive degree-days to be estimated from the monthly mean air temperatures, such as those provided by the CGCMs.

Ohmura (2001) asserted that a temperature-based melt index method is not inferior to methods based on the full spectrum of the energy balance, primarily because longwave downward radiation and sensible heat flux are strongly influenced by air temperature above the glacier. However, for a single glacier, the degree-day factor is usually a function of temperature and hence is climate dependent. Thus, to find an all-embracing degree-day factor for all the glaciers in GH is not a trivial task and may be even harder to calibrate (van der Veen 1999).

To estimate the ensemble behavior of glaciers, we introduce here a physically based method that explicitly introduces two atmospheric parameters that influence glacier mass balance, namely, temperature and wind speeds. Taking an area average of the continuity equation for individual glacier flow, the divergence of the ice-flux term diminishes and the only term that contributes to (spatially averaged) glacier thickness change is the surface mass balance (also spatially averaged). If we further average all glaciers residing in the GH, then change in accumulation caused by precipitation change plays a secondary role when compared with the enhanced ablation resulted from warming (e.g., Oerlemans 2005). Starting from the energy balance for a glacier residing on a sloped surface [based on the well-known energy balance equation of Budyko (1966); see the appendix], and then performing a linear perturbation analysis, and finally doing a scale analysis for a 1-K temperature increment, we obtain, to a first-order approximation, the following perturbation equation:

$$l\delta m = -\delta H, \tag{1}$$

where l is ice-melting latent heat (3.34×10^5 J kg^{-1}), m is the glacier mass balance, and H is the turbulent sensible heat flux. With H in Eq. (1) parameterized, a first-order estimation of the spatially averaged thickness change is

$$\frac{\partial h}{\partial t} = -\frac{\rho_a C_p \mathrm{K}_{h,2} U_2 (T_{a,2} - T_{\mathrm{sfc}})}{l\rho_i}, \tag{2}$$

where t is time and h is the spatially averaged glacier thickness (m). We use dh/dt to indicate the glacier-thinning rate (in ice-equivalent units). Here, we use the thickness change terminology in this context to indicate that the extra melting caused by a warming climate causes an overall thinning of the temperate glaciers. Here ρ_a is air density (kg m^{-3}), C_p is air heat capacity (1004 J kg^{-1} K^{-1}), K_h is stability-dependent bulk transfer coefficients for heat (unitless) at 2 m above ice surface, U is wind speed, T_a is air temperature (K), T_{sfc} is ground surface (skin) temperature, and ρ_i is ice density ($\sim 0.9 \times 10^3$ kg m^{-3} for a temperate glacier and smaller for dry glaciers at higher latitudes). The subscript 2 means 2 m above the ice surface. We used the climate value for $K_h = 1.6 \times 10^{-3}$, which is slightly smaller than the neutral value given by Andreas and Murphy (1986). This is a reasonable choice for a melting glacier surface [see section 5 of Hock (2005)]. Only ρ_a is assumed to be elevation dependent. For the same temperature increment and 2-m wind speed, a glacier at a lower elevation melts more quickly than at a higher elevation.

The problem of using a GCM-estimated T_{sfc} is that glaciers occupy only a very small fraction of a GCM grid box. Because of the huge temperature contrast between ice-covered and bare ground areas, the GCM-derived T_{sfc} may be several degrees higher than the actual temperature of the ice sheet. Used in Eq. (2), even the direction of the sensible heat flux cannot be guaranteed to be correct. The increment of the $T_{a,2}$ can, however, be used in Eq. (2) to estimate the superimposed melting rate, that is, the additional melting resulting from regional climate change. This is an especially sound assumption for the temperate glaciers, which have higher climate sensitivity than the dry subpolar glaciers and ice caps. Almost all glaciers outside the (sub)arctic regions are temperate, resulting from refreezing of meltwater penetrating into the snow (J. Oerlemans 2006, personal communication).

Because of the coarseness of the grid, CGCMs do not represent the detailed topography of the mountain areas. Through inversing a linear response equation and driving it with 169 glacier length records from different parts of the world, Oerlemans (2005) constructed temperature historical time series from year 1600 to 2000. He found that the warming signals extracted from glaciers at low and high elevations are similar, and further asserted that the warming in the lower troposphere appears to be elevation independent. Thus, the smoothed elevation as used in CGCMs appears not to be an important issue for estimating additional glacier melting from warming.

If the CGCM grid-box air temperature is representative of temperate glaciers, at least for JJA, we also can estimate the actual melting rates. In fact, the summer mean temperature is chosen from the consideration that, for the temperate glaciers, their surface in summer is not just temperate ice but a binary mixture of ice and water. This is the case at least for the lower part of the glacier, primarily resulting from refreezing of meltwater penetrating into the ice.

Like other approaches attempting to link the climate change signal to glacier behavior, this approach presented here is not intended to deal with surging glaciers, variations of which convey little information on climate change. The change in geometry of individual glaciers is not of concern for our gross estimations.

The steepness and orientation of the slopes play a central role in the local energy balance for a mountain glacier, especially for shortwave radiation. For example, at 45°N, gentle slopes (~0°–30°) of due south orientation enhance the JJA average shortwave radiation by ~0%–20%, relative to a flat surface, whereas north-facing slopes reduce the JJA average shortwave radiation by ~0%–55%. Thus, we use the surface-received shortwave radiation provided by the CGCMs and use it as for a flat surface. The longwave radiation depends weakly on slope steepness and orientation but strongly on elevation. The Bowen ratio estimation suggested in Andreas and Cash (1996) is suitable for a saturated ice/water surface. We adapted this scheme for partition of the net radiation (we did not include the salinity effect, though).

4. Results and discussion

After generalizing the effects of slope and orientation, as discussed in section 3, the base melting rates turn out to be primarily elevation dependent, with the 0.5 m yr^{-1} line coinciding with the 1500-m topography (Fig. 1a). This indicates also that the JJA warming under SRES A1B emission scenario is systematic in our region of interest. Using Eq. (2), with surface air temperature, skin temperature, surface air pressure, and wind speed all provided by MIROC3.2-hires simulations under SRES A1B scenario, we produced an environmental map for extra glacier melting for the future 30 yr. In Fig. 1b, regions with mean JJA surface temperature larger than 297 K are masked out from the practical consideration that summer temperatures as high as those values are very unfavorable for glaciers to survive. Figure 1b is a potential map because it does not actually predict the existence of a glacier. However, if a glacier is present at a particular location, regional warming over the next 30 yr under the SRES A1B scenario will reach our estimated melting rate, relative to a melting rate averaged over the years 2000–02.

For example, for the Tianshan–Altai Mountains region, warming will contribute about 0.15 m of glacier thinning each year. This is in agreement with the one-dimensional flow line model results of de Smedt and Pattyn (2003) for the Sofiyskiy glacier (49.78°N, 87.77°E), a low-elevation (medium elevation: 3200 m) glacier located in the Altai Mountains. Because of the low elevation, the warming from the last 30 yr has already moved the glacier far from a balanced state, because the volume reduction will be greater than 25% of its year 2000 value by year 2100 even if the current temperature remains constant. Additional temperature increases are primarily manifested as area shrinkage, because of the relatively flat glacier bed and the corresponding stronger front reaction. That is why they modeled a stronger dynamic sensitivity, expressed as a ratio of mass change to area change, of the Sofiyskiy glacier to the twenty-first-century's warming than that of many Alpine glaciers elsewhere. Further analysis indicates that the large surface temperature increase causes the maximum melting rate to be centered at the Tianshan–Altai region, whereas the associated wind speed increase contributes to the high-value region south of 30°N and between 80° and 105°E. This higher-resolution model also produces a maximum located around (40°N, 107°E), which the other two CGCMs of coarser resolution failed to identify. For most of the remaining Asian monsoon regions, the increase in melting rate is generally less than 0.1 m yr^{-1}.

We also repeated the above experiment for GFDL-CM2.1 (see Fig. 2) and the Met Office HadCM3 (Fig. 3). The elevation-dominated base-melting-rate maps (see Figs. 1a, 2a, and 3a) are similar among the three CGCMs, with more details revealed by MIROC3.2-hires, apparently resulting from its finer resolution of 1.125° latitude × 1.125° longitude. Although they have different spatial resolutions, HadCM3 (2.5° latitude × 3.75° longitude) and MIROC3.2-hires produce very similar patterns in additional melting for the GH region; there is a maximum centered on the Tianshan–Altai (42°N, 80°E) region, and another centered on the Hengduan Mountains (25°N, 100°E). For the Tianshan region, the magnitudes among the three also agree very well (~0.15 m yr^{-1}). For most of the regions, the GFDL-CM2.1 simulated an apparently weaker additional melting rate than the other two. The readers are cautioned that the spatial patterns in Figs. 1–3 might be

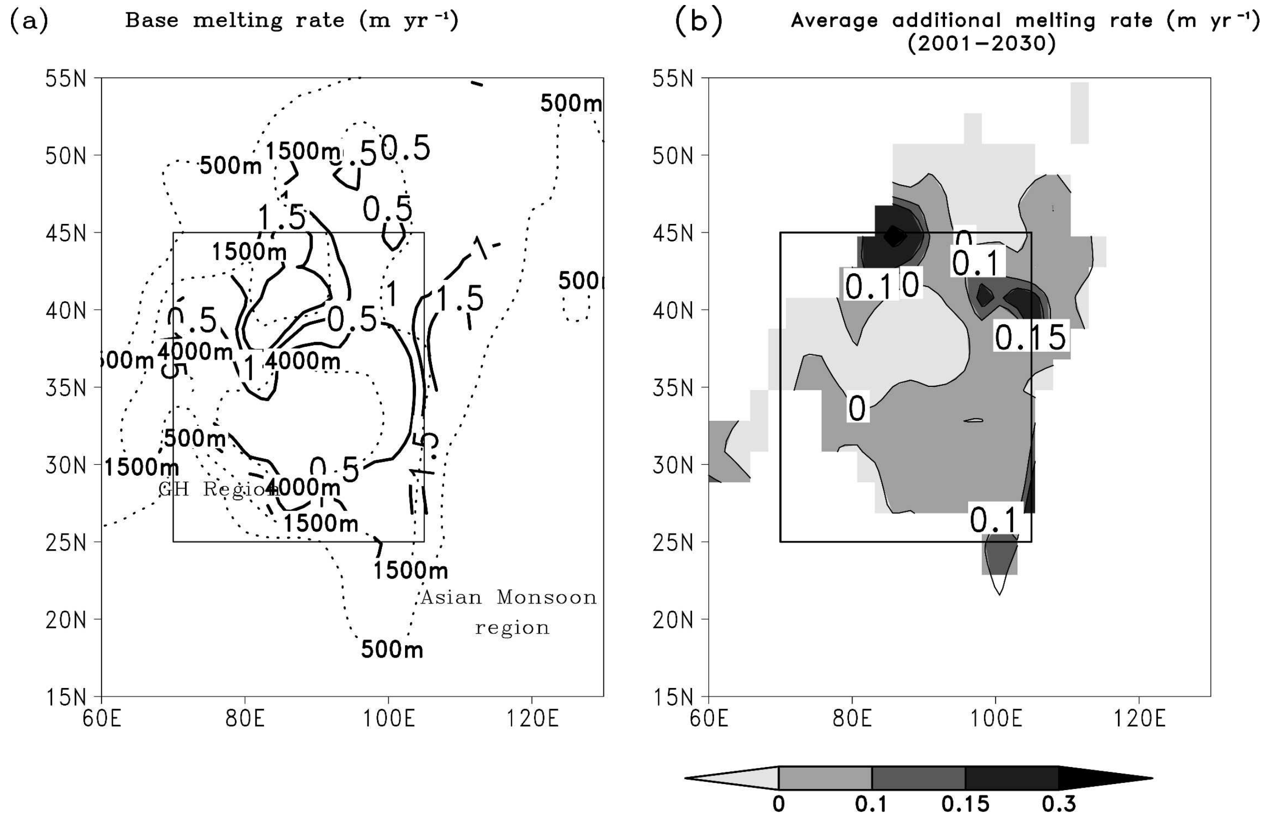

FIG. 2. As in Fig. 1, but for GFDL-CM2.1 simulations.

somewhat different from reality also because possible changes in precipitation are not included in Eq. (2).

To understand the temporal structure of the melting rate acceleration, an area average was taken within the GH to obtain the annual time series of the additional melt rate (Fig. 4). Although not completely in phase on an annual basis, the additional melting curves from three CGCMs appear to be very similar in that they show a general trend of gradual acceleration. The amplitude from GFDL-CM2.1 is smaller than that simulated by HadCM3 and MIROC3.2-hires. Averaged over the entire GH region, the accelerations in the melting rate are about 1, 3, and 5 mm yr^{-2} for GFDL-CM2.1, MIROC3.2-hires, and the Met Office HadCM3, respectively.

For the entire Asian monsoon region, as compared with possible variations in net radiation and precipitation in the 2001–30 period, the temperature variations play a first-order role in the glacier melting, as shown by Oerlemans (1994, 2005). Whether the estimations presented in Fig. 4 match reality depends primarily on the accuracy of the temperature scenarios. Despite its large rate, our CGCM estimates of the ice melting in the greater Himalayas still possibly are conservative, because we did not consider the following factors: (a) the positive feedback in net radiation used for melting, (b) the changes in precipitation form in the glacier source region, and (c) the dynamic response (movement) of the valley glacier.

The presence of liquid precipitation causes melting and is a negative factor in the glacier solid mass balance [see the Q_m term in Eq. (A1) in the appendix], because the heat transfer to snow by rain while cooling itself to 0°C is significant (Peng et al. 2002). This Q_m term may act in the following way for a warming climate. Increased temperatures will lead to a shift of the 0°C line, that is, the snow line, which generally is much higher than the glacier terminus, toward higher altitudes. Thus, the glacier receives lower monsoonal solid precipitation input to its mass balance during summer periods. Instead, the occurrence of rain precipitation at higher altitudes may lead to further reduction to the mass balance of a glacier. This concern is important because, as indicated by the circulation changes in the SRES A1B simulations from GFDL-CM2.1 (not shown here), the wind is strengthening in the future climate over the GH region, especially in the northern part. The next 30 yr could well be another wet phase, but within a warmer environment. The possibility of wetter summer months for the AM region also was reported

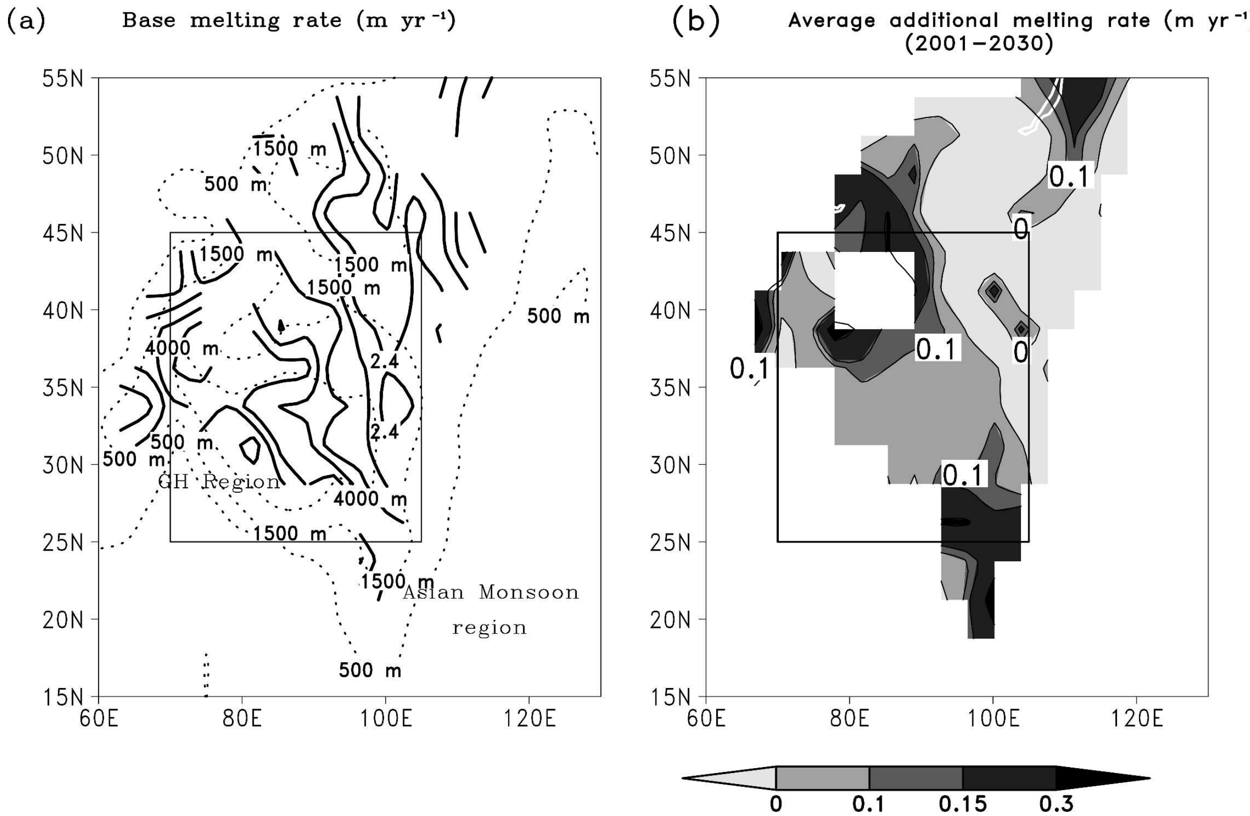

FIG. 3. As in Fig. 1, but for HadCM3 simulations.

by Kimoto (2005), based on the circulation changes under SRES A1B warming scenario. However, Duan et al. (2006) provided different accounts of the precipitation scenario in the Himalayas.

Because heat conduction within ice is a slow process, the time scale for dynamic responses of ice sheets to climate change (e.g., surface temperature) is estimated to be hundreds of years or greater (Alley and Whillans 1984). This is why we concentrated on surface melting. However, valley glaciers, which are common in our study region, tend to have crevasses that guide the surface meltwater to the bases, and thereby enhance the rate of downward movement of the glaciers. For valley glaciers, this mechanism is a positive feedback to melting, because of increases in the surrounding air temperature and air density [Eq. (2)]. The positive correlation between surface melting and the acceleration of the continental ice sheet was reported by Zwally et al. (2002).

5. Conclusions

As indicated in Oerlemans (1994), it is a huge task to handle all glaciers "in a single equation." In this study, we generalize one aspect of the response of glaciers to climate warming: the additional melting of temperate glaciers. In this study, by spatially averaging the mass continuity equation and carefully evaluating the energy balance terms for a sloped surface, we proposed a practical approach to the evaluation of the ensemble behavior of the GH glaciers in their additional thickness reduction responding to a warmer climate.

Three CGCMs give a consistent account of the mountain glacier melting under the SRES A1B scenario. For the mountain glaciers in the GH, our results show that the regions most affected by our CGCM calculations of global warming over the period of 2001–30 are the Tianshan–Altai and Hengduan Mountains, respectively due to significant warming and wind strengthening. A conservative estimate for these regions is that, for glaciers below an elevation of 4000 m, an additional 10-m thickness might be melted down by 2030. This result is especially significant because, as stated in the introduction, research on mountain glacier changes for these regions is still limited. Our CGCM results complement the remote sensing techniques used for glacier monitoring. To achieve higher spatial resolution, optical remote sensing techniques used for de-

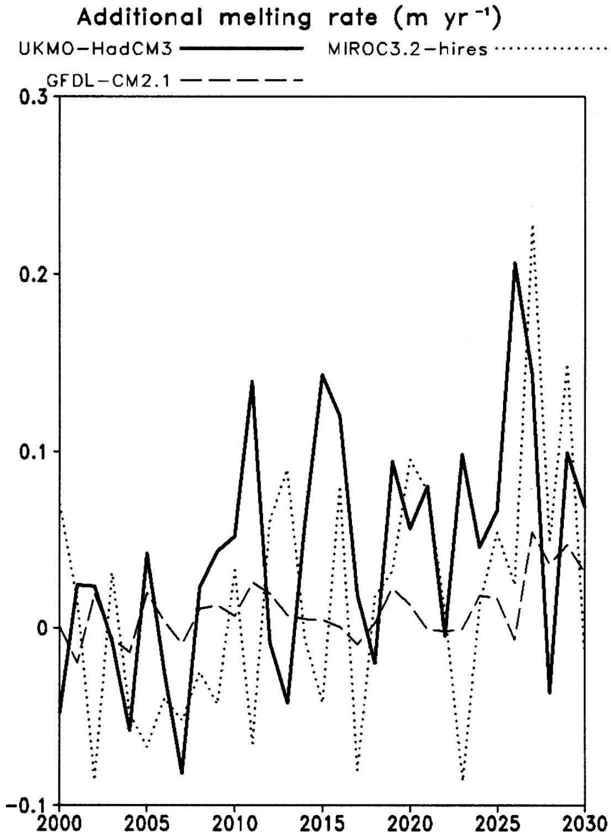

FIG. 4. Area-averaged additional melting rate simulated by three CGCMs for 2001–30.

tecting glacier variation primarily uses the visible bands, and therefore cannot measure the thickness and volume with acceptable accuracy (Davis et al. 1998). Airborne laser altimetry, which is used extensively to monitor the volume change of mountain glaciers, may provide data that can be used to verify the simple model used in this study.

If anthropogenic impacts on the earth's surface continue to accelerate, their effects on future climate are open to debate. However, even if the moderate emission scenario (SRES A1B) is realized in the future, mountain glaciers will most likely shrink rapidly, and it may actually take less than a century for the near-surface temperatures to rise to levels that threaten the existence of glaciers in the region. For surrounding regions with marginally enough freshwater supply, the loss of these "water towers," as a result of global warming, looms as a major environmental problem.

In this article we refrain from discussing precipitation effects, which are uncertain (see, e.g., the different results of Duan et al. 2006; Kimoto 2005) for the Asian monsoon region (which covers the GH). Changes in precipitation and the nivometric coefficient both depend on altitude as well as temperature and will be our next research goal. At present, we cannot assume that the CGCM output under the forcing scenarios is sufficiently reliable in its spatial and temporal variability estimation.

Acknowledgments. This work is supported by the Gary Comer Science Foundation. We acknowledge the international modeling groups for providing their data for analysis through the Intergovernmental Panel on Climate Change Data Archive at Lawrence Livermore National Laboratory. The first author is also thankful for useful discussions with Baolin Li from the Chinese Academy of Sciences. Our thanks are extended to an anonymous reviewer for reorganizing the presentation and making suggestions for future research. The authors thank J. Oerlemans for his valuable suggestions concerning the importance of temperate glaciers.

APPENDIX

The Energy Balance on Slopes

The energy balance on a sloped surface is

$$l = R_s + D_s + D_A + [(1 + \cos\alpha) + (1 - \varepsilon_f)\sin^2(\alpha/2)]\varepsilon_s \times \mathrm{LWD} - U_{\alpha-0} - \mathrm{OLR}_\alpha - (\mathrm{LE} + H + G) - Q_m, \tag{A1}$$

where R_s is the absorbed direct solar radiation including the slope and orientation effects, such as topographic shading; D_s and D_A are shortwave input from sky scattering and surrounding flat surface reflection; ε_s is emissivity of the slope; ε_f is emissivity of the flat surrounding surface; α is the slope angle; LWD is the downward longwave radiation; OLR_a is the outgoing longwave radiation; $U_{\alpha-0}$ is the radiative exchange between the slope and surrounding flat area; l is the latent heat used for ice melting; LE is latent heat used for evaporation of the liquid water or ice sublimation; H is the turbulent sensible heat exchange; G is the ground heat flux; and Q_m is advected heat flow (mass transfer of vapor or meltwater or rainwater) that applies during the rainy period and is significant for the glacier accumulation snow zone. We adopt the convention that all radiative terms [first six terms on the right-hand side of Eq. (A1)] are positive when they signify an energy gain for the sloped ground surface, whereas the remaining terms are positive when they deplete the energy of the sloped surface.

As the climate warms up, many factors emerge. In this study, we wish to identify the additional melting of valley glaciers as a result of temperature increases in the upcoming 30 yr. For this purpose, all feedbacks from solar radiation (e.g., effects from changing albedo, cloudiness as a result of large-scale circulation change, or land cover and soil moisture regime changes) are regarded as basic-state changes. For the monsoon region, the link between increased temperature and cloudiness is vague and beyond the scope of this research. Emissivity for snow and ice is close to unity and for most other natural surfaces are close to 0.98 and its variation is also omitted for the following analysis. For a glacier-covered slope, Eq. (A1) can be simplified by assuming ε_s as unity, with OLR_a being constant, and the reflectivity of the glacier does not vary as it melts.

Thus, a linear perturbation on Eq. (A1) reads,

$$\delta l = \left[(1 + \cos\alpha) + (1 - \varepsilon_f)\sin^2\frac{\alpha}{2}\right]\delta\mathrm{LWD} - 4\varepsilon_f\sigma T_f^3\delta T_f - (\delta\mathrm{LE} + \delta H + \delta G). \qquad \text{(A2)}$$

A scale analysis is performed on the above equation for a 1-K temperature increment. At the elevation of the glaciers (>3000 m), LWD is on the order of 150 W m^{-2} all year round, and a 1-K increment in air temperature means an approximimately 8 W m^{-2} increase in LWD. The second term, resulting from a differential temperature increment of the surrounding area and the slope (e.g., no increase in temperature for the glacier, but a 1-K increase of the surrounding rocks), is of the same order of an about 10 W m^{-2} increment in response to a 1-K increment. However, changes of sensible heat flux for a 1-K increment in air temperature are dependent on wind speed and are usually on the order of 80 W m^{-2} for such elevations and temperate climate zones. Because a glacier has a saturated surface, the partition of radiative energy into latent and sensible heat flux, that is, the Bowen ratio, is primarily temperature dependent (Andreas and Cash 1996). Because the melting surface keeps a 273.15-K temperature, the increase in air temperature creates larger moisture deficiency in the air and increases LE. However, an increment in LE is not the primary component of the latent heat flux increment; the increment in l is more significant. That is, the increased sensible heat flux received by the glacier is used primarily for melting, not for the evaporation of liquid water or sublimation. Thus, to a first-order approximation, the perturbation equation can be written as

$$\delta l = -\delta H. \qquad \text{(A3)}$$

Our energy balance equation is essentially the same as that used by Ohmura (2001). He justified the use of radiative components over the gross form of net radiation in the energy balance equation applicable for glaciers. As pointed out by a reviewer, Hock (2005) is an excellent resource for a review of the glacier melt models [combining his Eqs. (1) and (3) gives a formally identical expression to that of our Eq. (A1)].

REFERENCES

Ageta, Y., and K. Higuchi, 1984: Estimation of mass balance components of a summer accumulation type glacier in the Nepal Himalaya. *Geogr. Ann.,* **66,** 249–255.

——, and T. Kadota, 1992: Predictions of changes of glacier mass balance in the Nepal Himalaya and Tibetan Plateau: A case study of air temperature increase for three glaciers. *Ann. Glaciol.,* **16,** 89–94.

Alley, R. B., and I. M. Whillans, 1984: Response of the East Antarctica ice sheet to sea-level rise. *J. Geophys. Res.,* **89,** 6487–6493.

Andreas, E. L, and B. Murphy, 1986: Bulk transfer coefficients for heat and momentum over leads and polymyas. *J. Phys. Oceanogr.,* **16,** 1875–1883.

——, and B. A. Cash, 1996: A new formulation for the Bowen ratio over saturated surfaces. *J. Appl. Meteor.,* **35,** 1279–1289.

Braithwaite, R. J., 1984: Calculation of degree-days for glacier-climate research. *Z. Gletscherk. Glazialgeol.,* **20,** 1–8.

Budyko, M. I., 1966: Polar ice and climate. *Proceedings of the Symposium of the Arctic Heat Budget and Atmospheric Circulation,* J. Fletcher, Ed., Rand Corporation, 3–21.

Davis, C. H., C. A. Kluever, and B. J. Haines, 1998: Elevation change of the southern Greenland ice sheet. *Science,* **279,** 2086–2088.

Delworth, T. L., and Coauthors, 2006: GFDL's CM2 global coupled climate models. Part I: Formulation and simulation characteristics. *J. Climate,* **19,** 643–674.

de Smedt, B., and F. Pattyn, 2003: Numerical modelling of historical front variations and dynamic response of Sofiyskiy glacier, Altai Mountains, Russia. *Ann. Glaciol.,* **37,** 143–149.

Duan, K., T. Yao, and L. G. Thompson, 2006: Response of monsoon precipitation in the Himalayas to global warming. *J. Geophys. Res.,* **111,** D19110, doi:10.1029/2006JD007084.

Dyurgerov, M. B., and M. F. Meier, 1997: Mass balance of mountain and subpolar glaciers: A new global assessment for 1961–1990. *Arct. Alp. Res.,* **29,** 379–391.

Feddema, J. J., K. W. Oleson, G. B. Bonan, L. O. Mearns, L. E. Buja, G. A. Meehl, and W. M. Washington, 2005: The importance of land-cover change in simulating future climates. *Science,* **310,** 1674–1678.

Folland, C. K., and Coauthors, 2001: Global temperature change and its uncertainties since 1861. *Geophys. Res. Lett.,* **28,** 2621–2624.

Fu, C., H. Harasawa, V. Kasyanov, J. Kim, D. Ojima, Z. Wan, and S. Zhao, 2002: Regional-global interactions in East Asia. *Global–Regional Linkages in the Earth System,* P. Tyson et al., Eds., Springer, 109–149.

Gordon, C., C. Cooper, C. A. Senior, H. Banks, J. M. Gregory, T. C. Johns, J. F. B. Mitchell, and R. A. Wood, 2000: The simulation of SST, sea ice extents and ocean heat transports in a version of the Hadley Centre coupled model without flux adjustments. *Climate Dyn.,* **16,** 147–168.

Gregory, J. M., and Coauthors, 2005: A model intercomparison of changes in the Atlantic thermohaline circulation in response to increasing atmospheric CO_2 concentration. *Geophys. Res. Lett.,* **32,** L12703, doi:10.1029/2005GL023209.

Hock, R., 2005: Glacier melt: A review of processes and their modelling. *Prog. Phys. Geogr.,* **29,** 362–391.

Houghton, J. T., Y. Ding, D. J. Griggs, M. Noguer, P. J. van der Linden, X. Dai, K. Maskell, and C. A. Johnson, Eds., 2001: *Climate Change 2001: The Scientific Basis.* Cambridge University Press, 881 pp.

Karoly, D. J., and Q. Wu, 2005: Detection of regional surface temperature trends. *J. Climate,* **18,** 4337–4343.

Kimoto, M., 2005: Simulated change of the east Asian circulation under global warming scenario. *Geophys. Res. Lett.,* **32,** L16701, doi:10.1029/2005GL023383.

Lau, K.-M., and S. Yang, 1996: Seasonal variation, abrupt transition, and intraseasonal variability associated with the Asian summer monsoon in the GLA GCM. *J. Climate,* **9,** 965–985.

Luo, H., and M. Yanai, 1983: The large-scale circulation and heat sources over the Tibetan Plateau and surrounding areas during the early summer of 1979. Part I: Precipitation and kinematic analyses. *Mon. Wea. Rev.,* **111,** 922–944.

Meehl, G. A., and J. M. Arblaster, 1998: The Asian–Australian monsoon and El Niño–Southern Oscillation in the NCAR Climate System Model. *J. Climate,* **11,** 1356–1385.

Oerlemans, J., 1994: Quantifying global warming from the retreat of glaciers. *Science,* **264,** 243–245.

——, 2005: Extracting a climate signal from 169 glacier records. *Science,* **308,** 675–677.

Ohmura, A., 2001: Physical basis for the temperature-based melt-index method. *J. Appl. Meteor.,* **40,** 753–761.

Peng, G., L. Leslie, and Y. Shao, 2002: *Environmental Modeling and Prediction*. Springer, 480 pp.

Peterson, T. C., and R. S. Vose, 1997: An overview of the global historical climatology network temperature data base. *Bull. Amer. Meteor. Soc.,* **78,** 2837–2849.

Raper, S. C. B., and R. J. Braithwaite, 2006: Lower sea level rise projections from mountain glaciers and icecaps under global warming. *Nature,* **439,** 311–313.

Sheng, D., and C. Chen, 1996: Water resources of the Qinghai-Xizang Plateau and its exploitation. *J. Nat. Resour.,* **11,** 8–14.

Shi, Y., 2001: Estimation of the water resources affected by climatic warming and glacier shrinkage before 2050 in west China. *J. Glaciol. Geocryol.,* **23,** 333–341.

Thompson, L. G., and Coauthors, 1997: Tropical climate instability: The last glacial cycle from a Qinghai-Tibetan ice core. *Science,* **276,** 1821–1825.

——, T. Yao, E. Mosley-Thompson, M. E. Davis, K. A. Henderson, and P.-N. Lin, 2000: A high resolution millennial record of the south Asian monsoon from Himalayan ice cores. *Science,* **289,** 1916–1919.

van der Veen, C. J., 1999: *Fundamentals of Glacier Dynamics*. A. A. Balkema, 472 pp.

Yamada, T., T. Shiraiwa, T. Kadota, T. Watanabe, B. Rana, Y. Ageta, and H. Fushimi, 1992: Fluctuation of the glacier from the 1970s to 1989 in the Khumbu, Shorong and Langtang regions, Nepal Himalayas. *Bull. Glacier Res.,* **10,** 11–19.

Ye, D., 1981: Some characteristics of the summer circulation over the Qinghai-Xizhang (Tibet) Plateau and its neighborhood. *Bull. Amer. Meteor. Soc.,* **62,** 14–19.

Zwally, H. J., W. Abdalati, T. Herring, K. Larson, J. Saba, and K. Steffen, 2002: Surface melt-induced acceleration of Greenland ice-sheet flow. *Science,* **297,** 218–222.